Acta Pharmacologica Sinica

www.nature.com/aps

ARTICLE

Diosmetin has therapeutic efficacy in colitis regulating gut microbiota, inflammation, and oxidative stress via the circ-Sirt1/Sirt1 axis

Hai-long Li[1,2], Yi-ying Wei[1,2], Xiao-he Li[1,2], Shan-shan Zhang[1,2], Ruo-tong Zhang[1,2], Jin-he Li[1,2], Bo-wei Ma[1,2], Shuai-bo Shao[1,2], Zi-wei Lv[1,2], Hao Ruan[1,2], Hong-gang Zhou[1,2] and Cheng Yang[1,2]

Diosmetin (3',5,7 -trihydroxy-4'-methoxy flavone) is a natural flavonoid compound in the citrus species, it exhibits a variety of pharmacological activities, but little is known of its effects on colitis. In this study we evaluated the therapeutic effects of diosmetin on mouse models of chronic and acute colitis. Chronic colitis was induced in mice by drinking water containing 3% dextran sulfate sodium (DSS) from D0 to D8, followed by administration of diosmetin (25, 50 $mg \cdot kg^{-1} \cdot d^{-1}$) for another 8 days. Acute colitis was induced by drinking water containing 5% DSS from D0 to D7, the mice concomitantly received diosmetin (25, 50 $mg \cdot kg^{-1} \cdot d^{-1}$) from D1 to D7. During the experiments, body weight and disease activity index (DAI) were assessed daily. After the mice were sacrificed, colon tissue and feces samples were collected, and colon length was measured. We showed that in both models, diosmetin administration significantly decreased DAI score and ameliorated microscopic colon tissue damage; increased the expression of tight junction proteins (occludin, claudin-1, and zonula occludens-1), and reduced the secretion of proinflammatory cytokines IL-1β, IL-6, TNF-α, and Cox-2 in colon tissue. We found that diosmetin administration remarkably inhibited colon oxidative damage by adjusting the levels of intracellular and mitochondrial reactive oxygen species, GSH-Px, SOD, MDA and GSH in colon tissue. The protection of diosmetin against intestinal epithelial barrier damage and oxidative stress were also observed in LPS-treated Caco-2 and IEC-6 cells in vitro. Furthermore, we demonstrated that diosmetin markedly increased the expression of Nrf2 and HO-1 and reduced the ratio of acetylated NF-κB and NF-κB by activating the circ-Sirt1/Sirt1 axis, which inhibited oxidative stress and inflammation in vivo and in vitro. Diosmetin reversed the effects of si-circSirt1 and si-Sirt1 in LPS-treated Caco-2 and IEC-6 cells. When the gut microbiota was analyzed in the mouse model of colitis, we found that diosmetin administration modulated the abundance of Bacteroidetes, Actinobacteria, Cyanobacteria and Firmicutes, which were crucial for inflammatory bowel disease. Our results have linked colitis to the circ-Sirt1/Sirt1 signaling pathway, which is activated by diosmetin. The results imply that diosmetin may be a novel candidate to alleviate DSS-induced colitis and can be a lead compound for future optimization and modification.

Keywords: inflammatory bowel disease; colitis; diosmetin; proinflammatory cytokines; oxidative stress; gut microbiota

Acta Pharmacologica Sinica (2022) 43:919–932; https://doi.org/10.1038/s41401-021-00726-0

INTRODUCTION

Ulcerative colitis (UC), one of the main forms of inflammatory bowel disease (IBD), has severe clinical symptoms, such as diarrhea, abdominal pain, and bloody mucus in stool, which indicate a potential attack by cytokines [1, 2]. However, little is known about the pathogenesis of UC. Many studies reported that genetic factors, environmental factors, microbial factors, and molecules in the intestinal immune system have promoted the occurrence and development of UC [3]. The current pharmacological treatments for IBD are aminosalicylic acid and glucocorticoids, which cause serious side effects, including potential liver and kidney damage [4, 5]. Therefore, developing more effective therapeutic methods or agents and further investigating the underlying mechanisms of UC are important.

The intestinal epithelial barrier, composed of intestinal mucosa that connects epithelial cells and adjacent cells, is the first natural line of defense [6]. The pathogenesis of IBD is associated with intestinal epithelial barrier injury [7, 8]. Apical tight junction protein is a closed complex formed by the interconnection of transmembrane proteins (claudin and occludin) and perimembrane protein (zonula occludens-1 [ZO-1]), which is vital in the control of epithelial barrier function and the maintenance of paracellular permeability [9, 10]. Furthermore, inflammation and oxidative stress play critical roles in the pathogenesis of IBD. Reactive oxygen species (ROS) can induce intestinal tissue lipid peroxidation, intercellular junction disruption, and leukocyte and neutrophil infiltration, as well as promote the inflammatory process. The accumulation of ROS in the gut can cause the death

[1]The State Key Laboratory of Medicinal Chemical Biology, College of Pharmacy and Key Laboratory of Molecular Drug Research, Nankai University, Tianjin 300350, China and [2]High-throughput Molecular Drug Screening Centre, Tianjin International Joint Academy of Biomedicine, Tianjin 300350, China
Correspondence: Hong-gang Zhou (honggang.zhou@nankai.edu.cn)
These authors contributed equally: Hai-long Li, Yi-ying Wei, Xiao-he Li.

Received: 22 February 2021 Accepted: 22 June 2021
Published online: 14 July 2021

of mice and *Drosophila melanogaster* [11, 12]. Therefore, preventing ROS and proinflammatory cytokine accumulation in the gut may be able to alleviate IBD.

Studies on the relationship between disease and gut microbiota strongly indicated that gut microbiota play critical role in gut disorders, including IBD, obesity, liver disease, and colorectal cancer [13–15]. Imbalance in gut microbiota can directly disrupt tightly connected proteins, decrease the integrity of intestinal mucosa epithelium, and ultimately hurt the mucosal barrier [16, 17]. Moreover, gut microbiota can promote the differentiation of immune cells and the production of immune mediators, which regulate intestinal immune function [18]. Thus, looking into the possible effect of gut microbiota on IBD and seeking potential treatment are critical.

Silent information regulator 1 (Sirt1), a member of the sirtuin family that has been studied extensively and in-depth, plays important roles in anti-aging, apoptosis, oxidative stress, and DNA damage. The deacetylation of Sirt1 is an important component of anti-intracellular inflammatory response. Sirt1 interacts with NF-κB and inhibits the acetylation of NF-κB to inhibit transcription [19]. Sirt1 can also regulate the key transcription factor of oxidative stress, Nrf2, and therefore affects the redox state of cells [20]. Li et al. [21] revealed that Sirt1 prevents intestinal inflammation by regulating gut microbiota. Sirt1 regulates NF-κB and Nrf2 pathways and gut microbiota to maintain intestinal epithelial homeostasis as a transportation hub.

Circular RNA (circRNA), a covalently closed circular competitive internal RNA, participates in the regulation of the circRNA–miRNA–mRNA network and plays an important role in the regulation of various diseases, including colitis [22]. Fan demonstrated that CircKcnt2 inhibits ILC3 activation and alleviates the progression of colitis [23]. Intestinal immune cells promote the self-renewal of intestinal stem cells through circPan3 [24]. Moreover, circ-Sirt1 inhibits vascular inflammation by regulating NF-κB acetylation and the Sirt1 pathway [25]. Therefore, upregulating Circ-Sirt1 to increase Sirt1 signal may be a potential strategy against dextran sulfate sodium (DSS)-induced colitis.

Diosmetin (3',5,7-trihydroxy-4'-methoxy flavone, $C_{16}H_{12}O_6$) is a natural flavonoid compound found in the citrus species [26]. Diosmetin has activities against tumor, acute kidney injury, and acute lung injury [27–29]. Diosmetin can also attenuate oxidative stress and decrease the level of proinflammatory cytokine [30, 31]. In our experiment, we studied and reported the effects and potential molecular mechanisms of diosmetin in treating IBD.

MATERIALS AND METHODS

Animal and ethical approval

C57BL/6 mice (18–22 g, 4–6 weeks old) were obtained from the Experimental Animal Center at Nankai University (Tianjin, China; SCXK: 2019-0001). All animal care and laboratory procedures are approved by the Animal Care and Use Committee of Nankai University (IACUC) (License No. SYXK 2019-0001). The animals were maintained under a controlled environment (23 ± 2 °C, 50% ± 5% humidity, and 12 h/12 h light/dark cycle) with free access to food and water, and acclimatized for 1 week before the experiment.

DSS-induced IBD

The first model [32] was divided into five groups ($n = 8$): control group (0.5% sodium carboxymethyl cellulose [CMC-Na]), DSS group (3% DSS), DSS with salazosulfapyridine (SASP, 200 mg/kg) group, and DSS with diosmetin (25 and 50 $mg \cdot kg^{-1} \cdot d^{-1}$) group. The mice in the DSS, DSS with SASP, and DSS with diosmetin groups were given 3% DSS (molecular weight, 36–50 kDa; MP Biomedical Solon, OH, USA) in drinking water on days 0–7, and the daily drinking volume of each mouse was calculated as 6 mL. The DSS solution was supplemented to the daily drinking volume the next day. The mice in the control group were given drinking water without DSS. The mice in the DSS with SASP and DSS with diosmetin groups, were intragastrically administered SASP (200 $mg \cdot kg^{-1} \cdot d^{-1}$) and diosmetin (25 and 50 $mg \cdot kg^{-1} \cdot d^{-1}$) on the days 8–15, respectively, and the mice in the NC and DSS groups were given 0.5% CMC-Na. The second model [33] was also divided into five groups ($n = 8$): control group (0.5% CMC-Na), DSS group (5% DSS), DSS with SASP (200 $mg \cdot kg^{-1} \cdot d^{-1}$) group, and DSS with diosmetin group (25 and 50 $mg \cdot kg^{-1} \cdot d^{-1}$). The mice in the DSS, DSS with SASP, and DSS with diosmetin groups were given 5% DSS in drinking water on days 0–7, whereas the mice in the control group were given drinking water without DSS. The mice in the DSS with SASP and DSS with diosmetin groups were given SASP (50 $mg \cdot kg^{-1} \cdot d^{-1}$) and diosmetin (25 and 50 $mg \cdot kg^{-1} \cdot d^{-1}$) on days 1–7, respectively, and the mice in the NC and DSS groups were given 0.5% CMC-Na. During the experiments, body weight and disease activity index (DAI) [13] were measured daily. After the mice were sacrificed, colon tissue and feces samples were collected, and colon length was measured.

Histological assessment

The isolated colon tissues were fixed in 10% formalin for 1 week, embedded in paraffin, and sectioned into 5 μm slices. Then, the sections were stained with hematoxylin–eosin solution. Finally, images of the stained sections were photographed using a light microscope (Nikon Eclipse TE2000-U, Nikon, Tokyo, Japan). The samples were analyzed blindly by three independent reviewers in different cohorts to score the entire colon area. The pathological score of colon injury was assessed according to the morphological criteria described in previous studies [34].

Immunofluorescence assessment

The effect of diosmetin on ZO-1 expression was examined by immunofluorescence staining in vivo and in vitro. The tissue slices or formalin-fixed cells were incubated with anti-ZO-1 antibodies overnight at 4 °C, then washed three times with PBS, and incubated with fluorescein-conjugated secondary antibody for 1 h at 37 °C. The cell nuclei were stained with diaminidophenylindole (5.0 μg/mL). Finally, the samples were photographed using a confocal microscope (Nikon Eclipse TE2000-U, Nikon, Tokyo, Japan).

Cell viability assay

Caco-2 and IEC-6 cells were seeded in 96-well plates at a density of 5×10^4 cells/mL for 24 h and pretreated with various diosmetin concentrations (0–400 μM) for 6, 12, and 24 h and various lipopolysaccharide (LPS) concentrations (0–32 μg/mL). Cell viability was measured by MTT assay.

Measurement of transepithelial electrical resistance (TEER)

In vitro cell barrier integrity was assessed by measuring TEER. The TEER of Caco-2 and IEC-6 cells growing in transwell chambers was measured using EVOM2 (WPI, Sarasota, FL, USA) as previously reported [35]. The TEER values of Caco-2 and IEC-6 cells were measured daily. The cells entered a stable state (590 ± 15 $\Omega \cdot cm^2$) after 21 days of cell culture, which indicates that the in vitro barrier model was successfully established.

Measurement of permeability

Cell permeability was measured by fluorescein isothiocyanate (FITC)–dextran (40 kDa, Sigma-Aldrich) as previously described [36]. The original cell culture medium was discarded and replaced with phenol red-free minimal essential medium after 21 days of cell culture. FITC–dextran was added to the upper chamber to make the final concentration 1 mg/mL, and the cells were incubated at 37 °C for 4 h. Then, 100 μL of medium was extracted from the lower chamber to determine the fluorescence value. Fluorescence was detected using the Synergy H2 microplate

reader (Bio Tek Instruments, VT, USA) at 492 nm for emission and 520 nm for reception.

In vivo intestinal tissue permeability was also measured by FITC–dextran as described previously [37]. Briefly, mice were fasted overnight and given FITC–dextran (500 mg/kg) by gavage the next day. After 4 h, the serum of mice was collected and diluted at 1:5 with PBS (pH 7.4). Fluorescence was detected using the Synergy H2 microplate reader (Bio Tek Instruments, VT, USA).

Western blot

Total protein from Caco-2 and IEC-6 cells and colon tissues were homogenized using radioimmunoprecipitation assay lysis buffer containing protease and 1 mM phenylmethylsulfonylfluoride. The protein concentrations were tested using a Bicinchoninic Acid (BCA) Protein Assay Kit (Beyotime Institute of Biotechnology, Beijing, China) according to the manufacturer's protocol. The proteins were separated by sodium dodecyl sulfate–polyacrylamide gel electrophoresis (7.5%–15%) and then transferred to polyvinylidene fluoride membranes (Millipore, MA, USA). Finally, enhanced chemiluminescence was performed using a Bio-Spectrum Gel Imaging System (UVP, CA, USA). The experiments were replicated at least five times.

Quantitative real-time polymerase chain reaction (PCR) assay

Total RNA samples were obtained from colon tissues using TRIzol (Invitrogen, Carlsbad, CA, USA) reagent following the manufacturer's protocol. cDNA was synthesized through the reverse transcription of each RNA sample using First-Strand cDNA Synthesis SuperMix (TransGen Biotech, Beijing, China). The levels of proinflammatory factors were quantified using Green qPCR SuperMix (TransGen Biotech, Beijing, China). GAPDH RNA was used for normalization. The primers used in the present study are listed in Supplementary Table S1.

Biochemical analysis

The levels of glutathione peroxidase (GSH-Px), glutathione GSH, malondialdehyde (MDA), and superoxide dismutase (SOD) in colon tissues were determined using specific kits (Beyotime Institute of Biotechnology, Beijing, China) according to the manufacturer's instructions.

Intracellular ROS measurement

Caco-2 and IEC-6 cells were plated in 24-well culture plates at a density of 5×10^4 cells/mL and treated with diosmetin (25 and 50 μM) for 2 h before LPS challenge. Then, the cells were added with 500 μL of difluorescein diacetate (DCFH-DA, 10.0 μM) for the detection of ROS, which was photographed using a confocal microscope (LSM 800 with Airyscan, Jena, Germany).

Mitochondrial ROS determination

Caco-2 and IEC-6 cells were plated in 24-well culture plates at a density of 5×10^4 cells/mL and treated with diosmetin (25 and 50 μM) for 4 h before LPS challenge. Then, the cells were added with 1 mL of MitoSOX Red mitochondrial superoxide indicator (Yesen, Shanghai, China), incubated at 37 °C in the dark for 10 min, and washed three times with washing buffer. Finally, the cells were photographed using a confocal microscope (LSM 800 with Airyscan, Jena, Germany).

Microbial community analysis

Mice feces were collected and stored at −80 °C. The mice feces were divided into three groups ($n = 6$): control group, DSS group, and DSS with diosmetin (50 mg/kg) group. The feces samples were sent to Center for Genetic and Genomic Analysis (Microread Genetics, Co., Beijing, China) under dry ice conditions for 16S rDNA gene sequencing. The DNA of total bacteria in mice feces was extracted with QIAamp® Fast DNA Stool Mini Kit. Primers corresponding to the V3–V4 regions of bacterial 16S rRNA were selected for amplification. The sequencing results and statistical results of the sequence data of all samples were based on sequenced reads and operational taxonomic units (OTUs).

Statistical analysis

Data were expressed as mean ± standard deviation and analyzed using GraphPad Prism 7 (Graph Pad Software, Inc., San Diego, CA, USA). Statistical analysis was performed through one-way ANOVA when comparing multiple independent groups. $P < 0.05$ was considered statistically significant.

Materials

Diosmetin (purity >98%) was obtained from Shanghai Yuanye Bio-Technology Co., Ltd. (Shanghai, China). LPS was purchased from Santa Cruz Biotechnology (Santa Cruz, USA). The BCA Protein Assay Kit, DCFH-DA, GSH-Px, GSH, MDA, and SOD kits were obtained from Beyotime Institute of Biotechnology (Shanghai, China). The First-Strand cDNA Synthesis SuperMix Kit and Green qPCR SuperMix Kit were obtained from TransGen Biotech (Beijing, China). MitoSOX Red mitochondrial superoxide indicator was purchased from Yesen (Beijing, China). Anti-occludin, anti-claudin-1, and anti-ZO-1 were obtained from Proteintech Group, Inc. (Chicago, IL, USA). Anti-GAPDH was obtained from Cell Signaling Technology (Boston, USA).

RESULT

Diosmetin protects against DSS-induced colitis in vivo

We evaluated the effects of diosmetin on DSS (3% and 5%)-induced colitis. The experimental program is illustrated in Fig. 1a, b. The body weight of the mice decreased apparently and DAI score increased rapidly after 3% DSS treatment. These effects reverted when the administration of 3% DSS was stopped (Fig. 1c). Body weight increased and DAI score decreased in mice treated with diosmetin compared with the 5% DSS group, but the differences were not statistically substantial (Fig. 1d). Furthermore, colon length was remarkably shortened in the DSS group compared with the control group but became longer in the DSS with diosmetin group compared with the DSS group (Fig. 1e, f). Histopathological changes, including inflammatory infiltration, in the groups treated with DSS only were all markedly reversed by SASP and diosmetin (Fig. 1g, h). Moreover, diosmetin remarkably reduced the DSS-induced histopathological scores (Supplementary Fig. S1a, S1b).

The viability of Caco-2 and IEC-6 cells changed but without any remarkable difference compared with that of the control group after diosmetin treatment (25–400 μM) for 6–24 h (Supplementary Fig. S1c, S1e). This result revealed that diosmetin is nontoxic to Caco-2 and IEC-6 cells under such conditions. Exposure to LPS (0.125–32 μg/mL) for 24 h slightly changed the viability of Caco-2 and IEC-6 cells but without any substantial difference compared with the control group (Supplementary Fig. S1d, S1f). These results indicated that diosmetin markedly alleviates DSS-induced colitis and is nontoxic to Caco-2 and IEC-6 cells.

Diosmetin alleviates intestinal epithelial barrier damage in vitro and in vivo

We tested the effect of diosmetin on intestinal epithelial barrier damage in vivo and in vitro. Compared with the control group, the expression levels of tight junction proteins (occludin and claudin) in the DSS group were decreased; however, diosmetin and SASP were able to markedly increase the expression of occludin and claudin compared with the model group (Fig. 2a, b). The results of the immunofluorescence analysis of ZO-1 in Fig. 2c, d show that the expression levels of ZO-1 in colon sections markedly decreased after DSS treatment in vivo compared with the control group. However, ZO-1 expression was remarkably upregulated in the DSS with diosmetin and DSS with SASP groups (Fig. 2c, d). Compared with control groups, the serum FITC–dextran content of the DSS group was increased, which indicated intestinal leakage, whereas

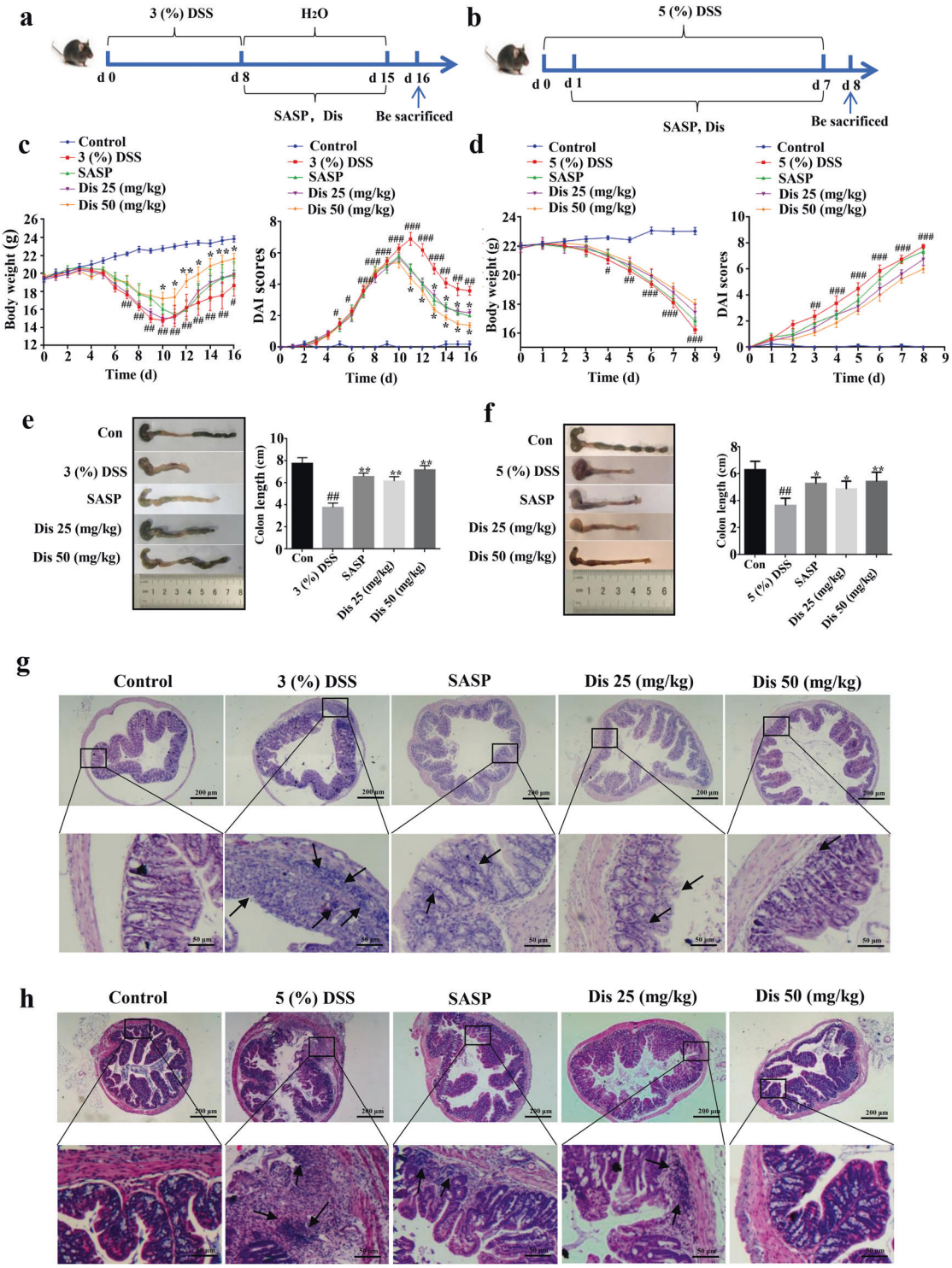

Fig. 1 Effects of diosmetin treatment on DSS-induced two mouse models of colitis. a Chronic colitis experimental procedure. **b** Acute colitis experimental procedure. **c** Effects of diosmetin on body weight and DAI score in chronic colitis. **d** Effects of diosmetin on body weight and DAI score in acute colitis. **e** Colon lengths in diosmetin-treated chronic colitis. **f** Colon lengths in diosmetin-treated Acute colitis. Histological sections of colonic tissue stained with hematoxylin and eosin are shown by microscope: **g** chronic colitis. **h** Acute colitis. Data are presented as the mean ± SD ($n = 8$). $^{\#}P < 0.05$, $^{\#\#}P < 0.01$, $^{\#\#\#}P < 0.001$, significantly different from control group; $^{*}P < 0.05$ and $^{**}P < 0.01$ significantly different from DSS groups.

that of the DSS with diosmetin group was remarkably inhibited (Fig. 2e, f). Next, we analyzed the expression of tight junction proteins, occludin and claudin, by Western blot after the 24 h exposure of Caco-2 and IEC-6 cells to different LPS concentrations (0.1–30 μg/mL). The expression levels of occludin and claudin in Caco-2 and IEC-6 cells obviously decreased in a dose-dependent way in the LPS-treated group (Fig. 3a). Furthermore, the expression levels of occludin and claudin remarkably decreased when administered with LPS (30 μg/mL). The expression levels of occludin and claudin in Caco-2 and IEC-6 cells obviously increased

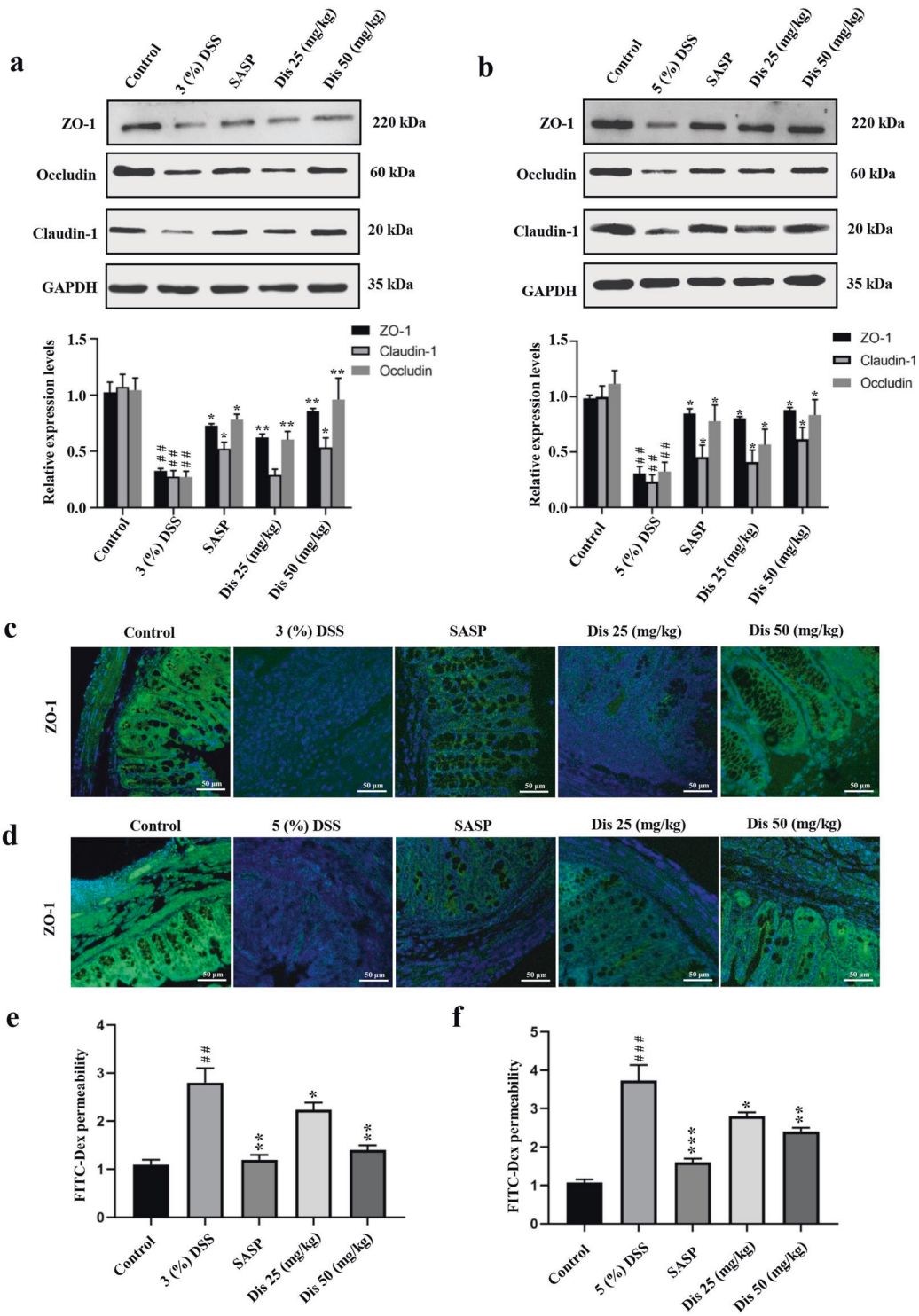

Fig. 2 Diosmetin regulates the tight junction proteins expression in vivo. a Effects of diosmetin on the protein levels of Occludin and Claudin-1 in chronic colitis. **b** Effects of diosmetin on the protein levels of Occludin and Claudin-1 in Acute colitis. **c** Effects of diosmetin on the expression levels of ZO-1, based on immunofluorescence staining in chronic colitis. **d** Effects of diosmetin on the expression levels of ZO-1, based on immunofluorescence staining in acute colitis. **e**, **f** The permeability of intestinal epithelial cells in different in vivo models was detected by FITC-glucan. Data are presented as the mean ± SD ($n = 5$). $^{\#\#}P < 0.01$, $^{\#\#\#}P < 0.001$, significantly different from control group; $^{*}P < 0.05$, $^{**}P < 0.01$, and $^{***}P < 0.001$ significantly different from DSS groups.

after treatment with diosmetin (25–100 ng/mL) for 24 h (Fig. 3b). The immunofluorescence analysis of ZO-1 exhibited similar results (Fig. 3c, d). Consistently, the Caco-2 and IEC-6 cells treated with diosmetin had increased TEER values (Fig. 3e) and decreased paracellular permeability for FITC–dextran (Fig. 3f).

Diosmetin reduces proinflammatory cytokines in vivo

Reducing inflammatory cytokines is a logical treatment for IBD. The effects of diosmetin on the expression of inflammation-related genes were studied at the mRNA level (Fig. 4). Diosmetin (50 mg/kg) significantly ($P < 0.05$) inhibited the expression of IL-1β,

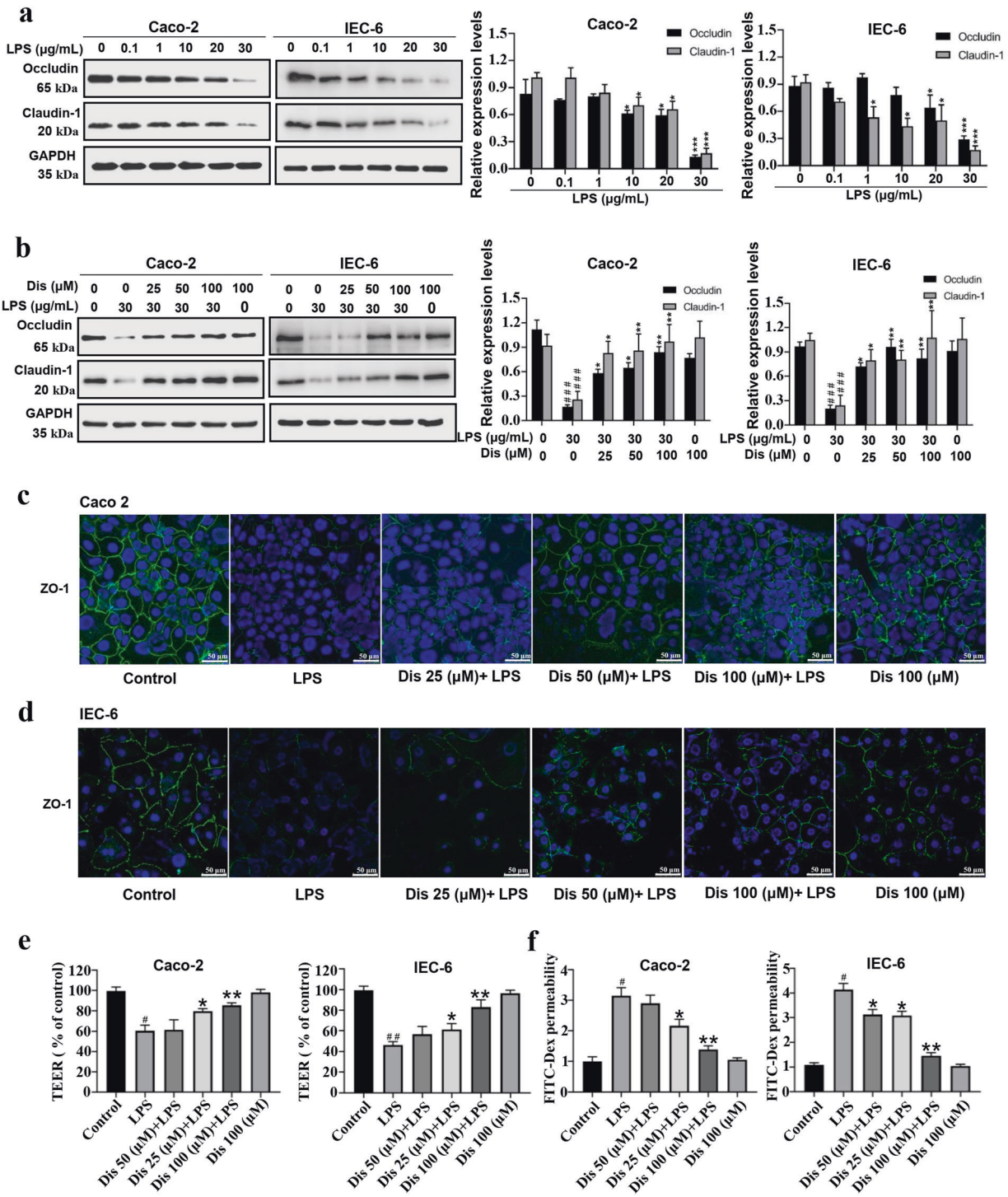

Fig. 3 Effects of diosmetin on protecting against LPS-induced damage of the epithelial barrier in Caco-2 and IEC-6 cells. a Dose-dependent effect of LPS on expression of proteins Occludin and Claudin-1 in Caco-2 and IEC-6 cell. **b** Effects of diosmetin on the protein levels of Occludin and Claudin-1 in Caco-2 and IEC-6 cells. **c**, **d** Effects of diosmetin on ZO-1 levels based on immunofluorescence staining in Caco-2 and IEC-6 cells. **e** TEER values of Caco-2 and IEC-6 cells were determined 24 h after LPS or diosmetin administration, respectively. **f** The permeability of Caco-2 and IEC-6 cells was detected by FITC-glucan. Data are presented as the mean ± SD ($n = 3$). $^{\#}P < 0.05$, $^{\#\#\#}P < 0.001$, significantly different from control group; $^{*}P < 0.05$, $^{**}P < 0.01$ and $^{***}P < 0.01$ significantly different from LPS groups.

IL-6, COX-2, and IFN-γ compared with the 3% DSS (Fig. 4a–d) and 5% DSS groups (Fig. 4e–h).

Diosmetin suppressed oxidative stress in vitro and in vivo

Inflammation stimulates the production of ROS, and ROS further increases the release of inflammatory mediators, such as cytokines and chemokines, which lead to epithelial cell damage, aggravation of oxidative stress, and the destruction of the intestinal barrier. Therefore, we tested the effect of diosmetin on active oxygen. Compared with the DSS (3% and 5%) groups, MDA levels in colon tissues were remarkably decreased and the levels of SOD, GSH, and GSH-Px were increased by diosmetin (Fig. 5a–h). The

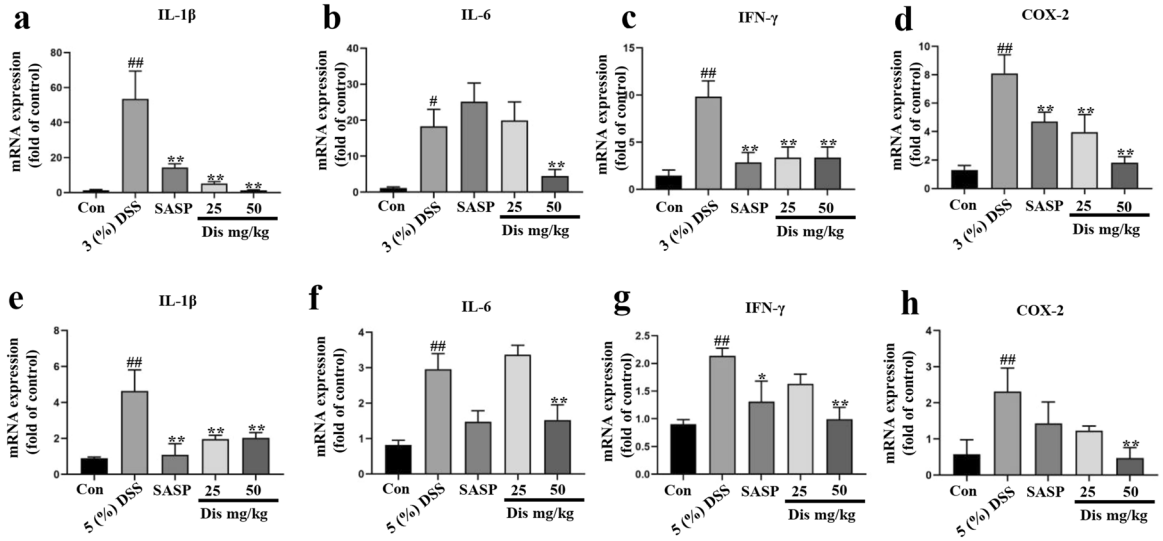

Fig. 4 Effects of diosmetin on the expression of inflammatory cytokines in colon tissue. Effect of diosmetin on inflammatory factors in acute colitis, **a** IL-1β; **b** IL-6; **c** IFN-γ; **d** COX-2. Effect of Dis on inflammatory factors in chronic colitis, **e** IL-1β; **f** IL-6; **g** IFN-γ; **h** COX-2. Data are presented as the mean ± SD ($n = 5$). $^{\#}P < 0.05$, $^{\#\#}P < 0.01$, significantly different from control group; $^{*}P < 0.05$ and $^{**}P < 0.01$ significantly different from DSS groups.

intracellular ROS levels of Caco-2 and IEC-6 cells in the LPS group remarkably increased compared with that of the control group. However, diosmetin considerably decreased the ROS levels in Caco-2 and IEC-6 cells compared with the LPS group (Fig. 5i, j). Next, we evaluated the mitochondrial ROS production. Compared with the LPS group, diosmetin markedly decreased the mitochondrial ROS levels of Caco-2 and IEC-6 cells (Fig. 5k, l).

Effects of diosmetin and DSS on gut microbiota

Different alpha diversity indices of each sample, including Shannon–Wiener curve, Simpson index, PD_whole_tree index, Good's_coverage index, Chao1 index, observed_species index, and rank abundance curve, are near flat (Supplementary Fig. S2), which indicates that the bacterial diversity and sequencing depth were sufficient. The alpha diversity indexes of the DSS group observably decreased ($P < 0.05$) compared with the control group; however, the diversity of the DSS with diosmetin group markedly increased compared with the DSS group (Fig. 6a–f). The USearch61 clustering algorithm in the QIIME software was used to group the sequences into multiple OTUs with 97% sequence similarity. We found 1629 unique OTUs in the control group, 536 in the DSS group, and 397 in the DSS with diosmetin group (Fig. 6g). The results of beta diversity analysis and principal component analysis (PCA) are displayed in Fig. 6h, and the result of the UniFrac heatmap analysis is displayed in Supplementary Fig. S3. UniFrac analysis was performed using weighted and unweighted UniFrac. Unweighted UniFrac can detect the existence of variation between samples, whereas weighted UniFrac can quantitatively detect the variation that occurs on different lineages between samples. PCA and UniFrac heatmap analysis showed that DSS considerably changed the gut microbiota, and diosmetin could regulate the gut microbiota. The DSS group had a decreased relative abundance of Bacteroidetes and Cyanobacteria and an increased relative abundance of Firmicutes compared with the control group in the phylum level; however, the DSS with diosmetin group had an increased relative abundance of Bacteroidetes and Cyanobacteria and a decreased relative abundance of Firmicutes compared with the DSS group (Fig. 6i).

The relative abundance of Lachnospiraceae and Ruminococcaceae markedly decreased and the relative abundances of Bacteroidaceae, Clostridiaceae, Lactobacillaceae, and Turicibacteraceae remarkably increased after DSS treatment compared with the control group (Supplementary Figs. S4 and S5). The whole-sample microbial community structure was analyzed by species abundance clustering heatmap at the phylum level (Supplementary Fig. S6).

Least discriminant analysis effect size (LEfSe) analysis was used to discover high-dimensional biomarkers and genomic features to find marker bacteria with statistical differences among the groups. Non-parametric factorial Kruskal–Wallis sum-rank test was used to detect features and taxa with substantial differences in abundance [38]. The results show 42 dominant OTUs from the three groups. Herein, three distinct OTUs were observably reversed by diosmetin intervention (Supplementary Fig. S7a). This result is also shown in the evolutionary branch graph of the LEfSe analysis (Supplementary Fig. S7b). Diosmetin treatment markedly decreased the abundance of *Eggerthella, Flavobacterium*, and *Clostridium* and remarkably increased the abundance of Odoribacteraceae, *Prevotella*, Rikenellaceae, *Ruminococcus, Coprococcus, Roseburia, Oscillospira, Anaeroplasma and* Synergistales compared with the DSS group (Supplementary Fig. S8).

Furthermore, PICRUSt was used to predict the discrepancy in the functional profiles between different groups (Supplementary Fig. S9). Compared with the DSS group, 14 (eight enriched, six depleted) functional modules were significantly altered ($P < 0.05$) by diosmetin treatment. Diosmetin caused changes in some metabolism pathways, such as the arginine, ornithine, and proline interconversion; methanogenesis from acetate; and the superpathway of tetrahydrofolate biosynthesis. In conclusion, these data illustrated that diosmetin contributes to the functional difference in gut microbiota.

Diosmetin inhibits NF-κB acetylation and promotes the Nrf2 pathway by activating the circSirt1/Sirt1 axis

We first detected the expression of circ-Sirt1 by qRT-PCR to verify the mechanism of diosmetin in relieving colitis. Diosmetin can dose-dependently alleviate the inhibition of circSirt1 by DSS or LPS in vitro and in vivo (Fig. 7a–d). We used the end-to-end sequence of mouse Sirt1 mRNA exons 2–7 to design forward and reverse primers. The RT-PCR product was purified and sequenced to confirm the circ-Sirt1 connection sequence and confirm the presence of circSirt1 in mouse colon tissue (Fig. 7e). Diosmetin remarkably increased the expression of Sirt1, Nrf2, HO-1, and nucleus Nrf2 and decreased the ratio of acetyl NF-κB and NF-κB

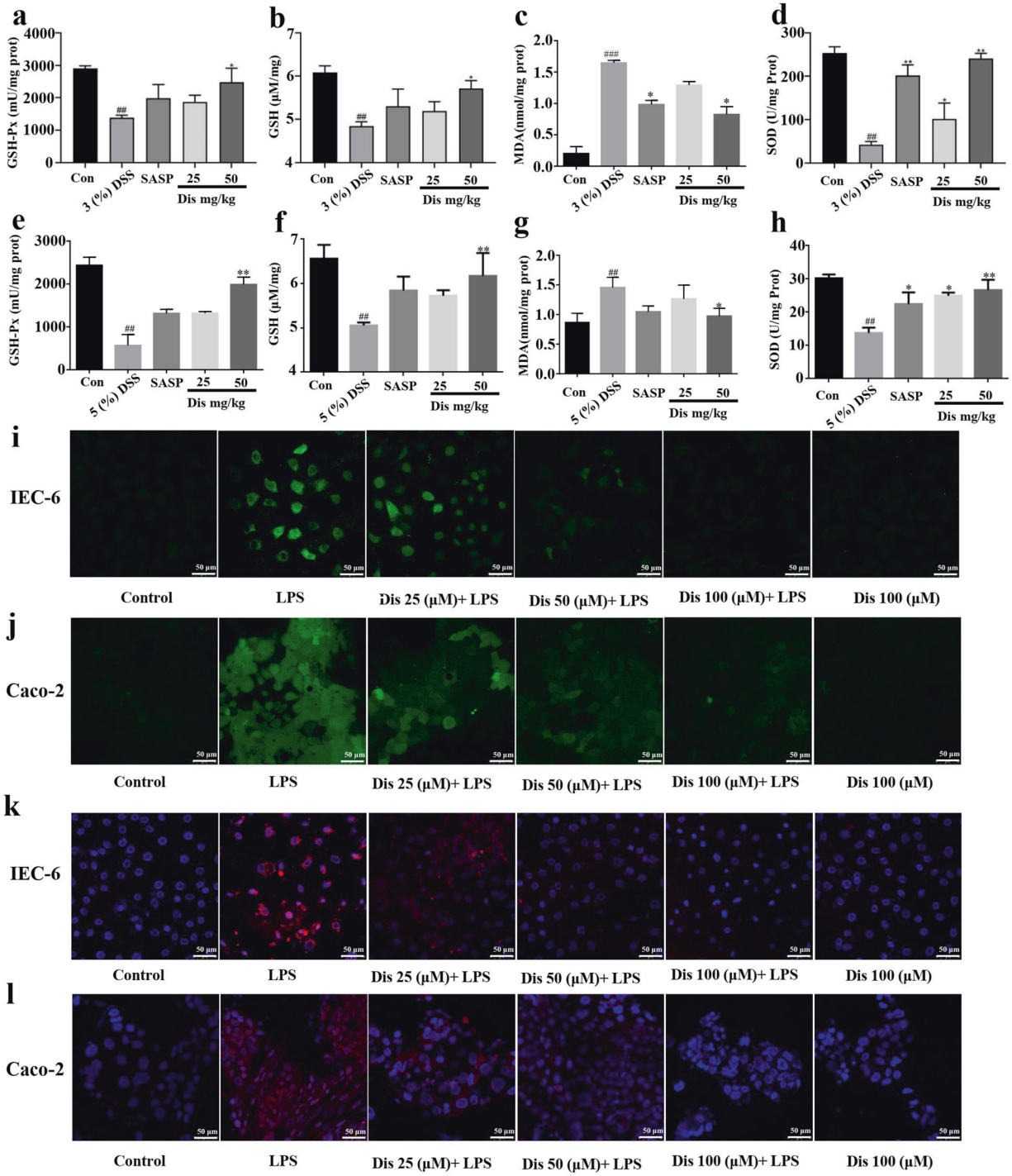

Fig. 5 Effects of diosmetin on DSS-induced oxidative stress in vivo. Effects of Dis on **a** GSH-Px, **b** GSH, **c** MDA, and **d** SOD levels in colon tissues from chronic colitis. Effects of diosmetin on **e** GSH-Px, **f** GSH, **g** MDA and **h** SOD levels in colon tissues from acute colitis. **i**, **j** Effects of diosmetin on ROS level in LPS-treated IEC-6 and Caco-2 cells. **k**, **l** Effects of diosmetin on MitoSOX level in LPS-treated IEC-6 and Caco-2 cells. Data are presented as the mean ± SD ($n = 5$). $^{\#\#}P < 0.01$, significantly different from control group; $^{*}P < 0.05$ and $^{**}P < 0.01$ significantly different from DSS groups.

in vivo and in vitro (Fig. 8a–d). These data suggested that diosmetin inhibits inflammation and oxidative stress by activating the circ-Sirt1/Sirt1 axis.

Diosmetin reverses the effects of si-circ-Sirt1 and si-Sirt1

We speculated that the beneficial effects of diosmetin may be achieved by upregulating the Sirt1 signaling pathway through circ-Sirt1 to explore the mechanisms of the anti-inflammatory, antioxidant, and gut microbiota-regulating effects of diosmetin. Before the LPS test, Sirt1 siRNA and si-circ-Sirt1 were transfected into IEC-6 and Caco-2 cells, and the cells were pretreated with diosmetin (100 μM) for 4 h to test the hypothesis. Si-circ-Sirt1 remarkably inhibited the level of circ-Sirt1 in IEC-6 and Caco-2 cells (Supplementary Fig. S10). Compared with the si-NC group, the si-

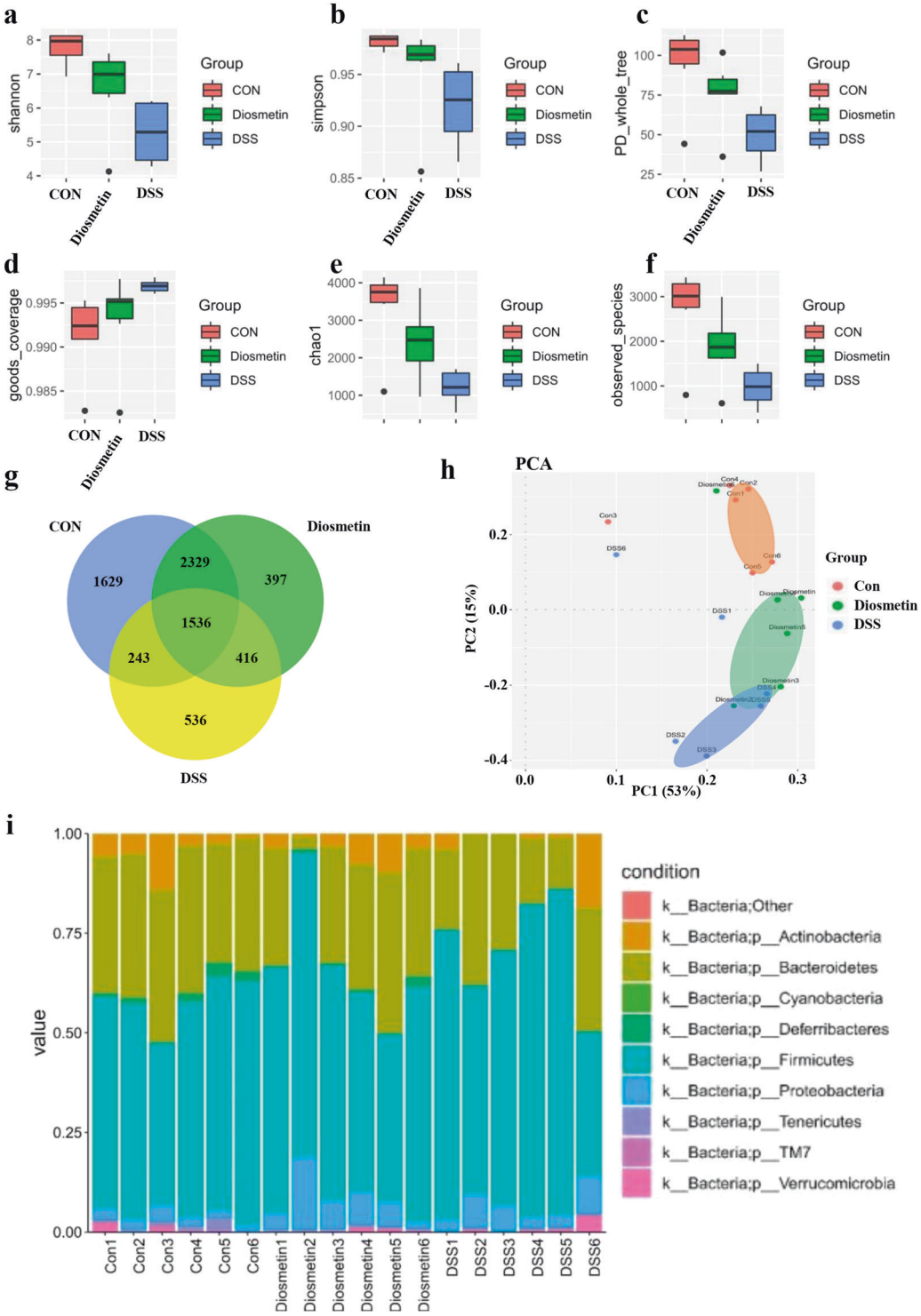

Fig. 6 Diosmetin modulates the gut microbiota composition induced by DSS-induced colitis. Comparison of alpha diversity accessed by **a** Shannon indexes; **b** simpson indexes; **c** PD_whole_tree; **d** good_coverage; **e** chao1 and **f** observed_species. **g** Unique organisms observed in the Control, DSS and Diosmetin groups. **h** PCA of gut microbiota communities based on OUT level in the Control, DSS and Diosmetin groups. The closer the distance between the two points, the smaller the difference in community composition between the two samples. **i** Column diagram of microbial composition at phylum level of each mouse.

circ-Sirt1 transfection group promoted the LPS-induced reduction of Sirt1 (Fig. 9a). Compared with the LPS group, si-circ-Sirt1 remarkably decreased the expression of Sirt1 and Nrf2 and increased the expression of Ac-NF-κB, whereas diosmetin remarkably reversed the effects of si-circ-Sirt1 (Fig. 9b). Compared with the LPS group, si-Sirt1 substantially decreased the expression of Sirt1 and Nrf2, and increased the expression of Ac-NF-κB, whereas diosmetin considerably reversed the effects of si-Sirt1 (Fig. 9c). These data suggested that diosmetin can reverse the effects of si-circ-Sirt1 and si-Sirt1 and regulates gut microbiota, inflammation, and oxidative stress through the circ-Sirt1/Sirt1 pathway (Fig. 9d).

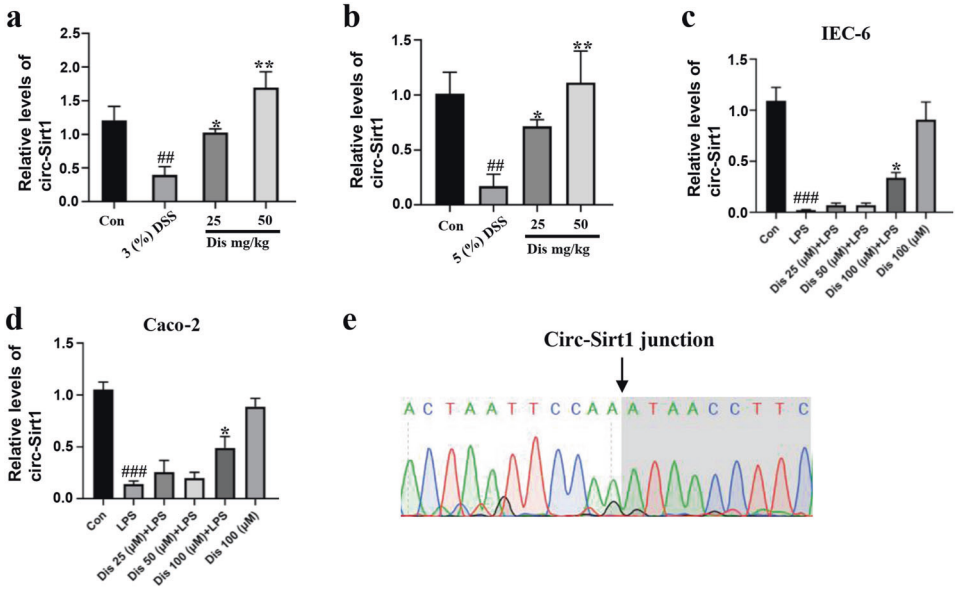

Fig. 7 Diosmetin modulate the expression of circ-Sirt1 in vivo and in vitro. a, **b** Effects of diosmetin on circ-Sirt1 levels of 3% DSS or 5% DSS-induced colitis in mice ($n = 5$). **c**, **d** Effects of diosmetin on circ-Sirt1 levels of LPS-induced IEC-6 and Caco-2 cells ($n = 3$). **e** RT-PCR products from mice were purified and sequenced. Data are presented as the mean ± SD. $^{\#\#}P < 0.01$ and $^{\#\#\#}P < 0.001$, significantly different from control group; $^{*}P < 0.05$ and $^{**}P < 0.01$ significantly different from DSS groups or LPS groups.

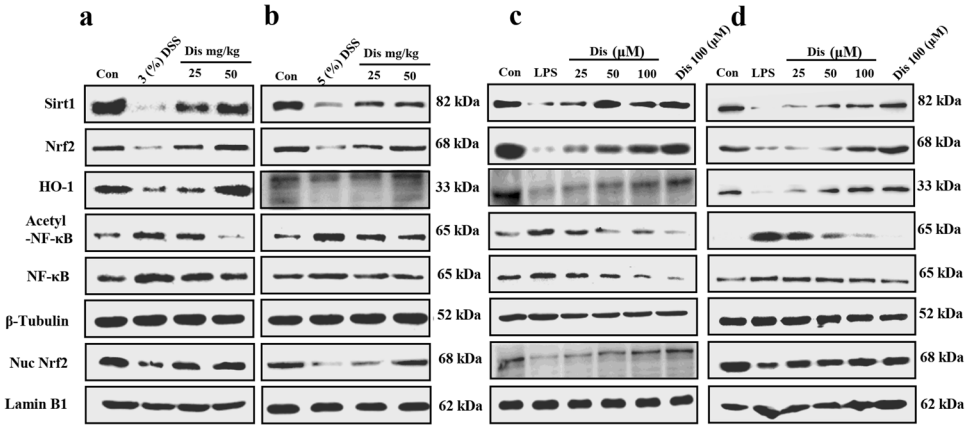

Fig. 8 Diosmetin regulates the Sirt1/Nrf2 and Sirt1/NF-κB mediated pathway in vivo and in vitro. a, **b** Effects of diosmetin on the protein levels of Sirt1, total Nrf2, nuclear Nrf2, HO-1, Acetyl-NF-κB, and NF-κB in colon tissues from mice ($n = 5$). **c**, **d** Effects of diosmetin on the protein levels of Sirt1, total Nrf2, nuclear Nrf2, HO-1, Acetyl-NF-κB, and NF-κB in IEC-6 and Caco-2 cells ($n = 3$).

DISCUSSION

DSS-induced colitis results in colon dysfunction, including severe intestinal barrier dysfunction, inflammatory infiltration, rectal bleeding, diarrhea, and gut microbiota changes [39–41], which are similar to the clinical and histological manifestations of human UC [42]. Antioxidants work against colitis by reducing inflammation and rebalancing gut microbiota [13, 33]. In this study, we adopted in vivo acute and chronic colitis mouse models induced by DSS (3% and 5%).

Diosmetin exerts protective effects against colon cancer and LPS-induced acute lung injury [28, 43]. The present study illustrated that diosmetin can protect against LPS-induced injury in Caco-2 and IEC-6 cells in vitro and against DSS-induced colitis in mice in vivo by alleviating histopathological changes and restoring the length of the colon. These data suggested that diosmetin can inhibit DSS-induced colitis.

The disruption of the intestinal epithelial barrier is related to colitis [44] and can lead to pathogenic antigen invasion. Thus, new ways of repairing mucosal barrier, improving mucosal healing, and reducing mucosal permeability are considered potential methods of treating colitis. Among many proteins in the mucosal barrier, ZO-1 is a major tightly linked scaffold protein associated with epithelial integrity [45], occludin is essential for barrier function and tight junction stability [46], and claudin-1 is a transmembrane protein and a component of tight junction strands [47]. Transmembrane proteins, claudin and occludin, and perimembrane protein, ZO, form a closed complex. The complex formation and breakage of ZO-1, claudin-1, and occludin in intestinal mucosal epithelial cells can greatly affect the function of the intestinal epithelial barrier [48]. In our study, the expression levels of claudin-1 and occludin were remarkably increased by diosmetin in vitro and in vivo compared with the DSS group. The expression of ZO-1 in immunofluorescence also remarkably increased by diosmetin in vitro and in vivo compared to DSS group. These data showed that diosmetin could inhibit DSS-induced intestinal epithelial barrier dysfunction.

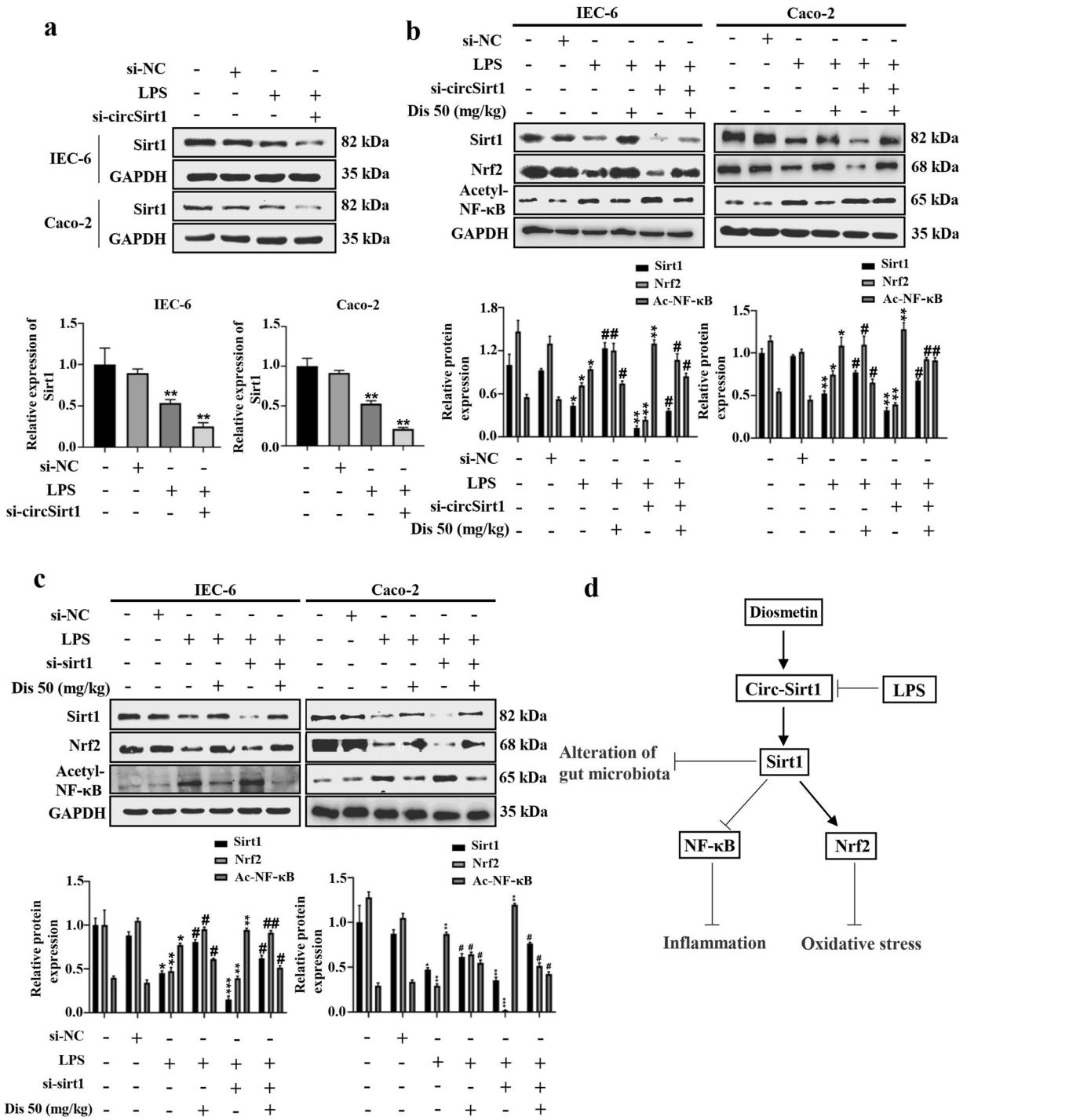

Fig. 9 Diosmetin reverses the effects of si-circSirt1 and si-Sirt1. a Effects of si-circSirt1 on Sirt1 protein levels in LPS-induced Caco-2 and IEC-6 cells. **b** The effect of diosmetin on the levels of Sirt1, Nrf2, and acetylated NF-κB protein after transfection of Caco-2 and IEC-6 cells with si-circ-sirt1. **c** The effect of diosmetin on the levels of Sirt1, Nrf2 and acetylated NF-κB protein after transfection of Caco-2 and IEC-6 cells with si-sirt1. **d** Schematic diagram of circSirt1/Sirt1 pathway promoted by diosmetin. Data are presented as the mean ± SD ($n = 3$). $^{\#}P < 0.05$ and $^{\#\#}P < 0.01'$ significantly different from LPS or LPS + si-circSirt1 or LPS + siSirt1 group; $^{*}P < 0.05$, $^{**}P < 0.01$, $^{***}P < 0.001$ significantly different from si-NC groups.

Oxidative stress and inflammation are related to DSS-induced colitis [49, 50]. MDA is a natural product of the lipid hydroperoxidation of organisms. Oxidative stress causes the oxidation and breakage of some fatty acids in cells into a series of compounds, including MDA, which has been used as an indicator of oxidative stress [51]. SOD is an important antioxidant enzyme that can catalyze disproportionate superoxide anions to generate H_2O_2 and O_2 [52]. GSH and GSH-Px can catalyze hydrogen peroxide and other peroxides to produce water and organic alcohol [53]. In our study, we found that DSS promoted oxidative stress as shown by the low levels of GSH, GSH-Px, and SOD and the high level of MDA in the colon tissue of mice, and these changes were reversed by diosmetin. In addition, diosmetin remarkably reduced the intracellular and mitochondrial ROS in Caco-2 and IEC-6 cells

caused by DSS. Therefore, inhibition of oxidative stress may be the mechanism by which diosmetin protects against DSS-induced colitis.

The inflammatory cytokines, IL-1β, IL-6, and IFN-γ, play leading roles in the formation of colitis [54]. In addition, these proinflammatory cytokines can stimulate the activation of NF-κB transcription [52]. The NF-κB pathway further releases proinflammatory cytokines, including TNF-α, IL-1β, and IL-6, in DSS-induced colitis [55]. IL-6 can stimulate the secretion of electrolytes from intestinal epithelial cells, which increases the permeability of endothelial cells, prompts the aggregation of neutrophils to the inflammation site, and causes IBD [56]. Yamamoto [57] demonstrated that the expression of IL-1β in the lesion site of UC is remarkably higher than that in the normal site; Yamamoto also found that the gene polymorphisms of IL-1β and IL-1RN are related to the genetic susceptibility and hormone dependence of UC. COX-2 plays a dominant role in the regulation of inflammatory state by stimulating the biosynthesis of prostaglandins [58]. IFN-γ is a mediator of the development of DSS-induced colitis [59]. Thus, the suppression of these inflammatory cytokines is an important target for the treatment of IBD. Our study found that diosmetin remarkably downregulated the mRNA levels of IL-1β, IL-6, COX-2, and IFN-γ, which suppress inflammation signaling pathways. These pathways may be the pathways of diosmetin against DSS-induced colitis.

Gut microbiota is a key factor in the pathogenesis of IBD [60, 61]. Robert W. Li's study of a porcine colitis model provided mechanistic insights into the attenuation of intestinal inflammation and the modulation of gut microbiome by krill oil [62]. In DSS-induced mouse colitis model, Lactobacillaceae remarkably inhibits the activation of NF-κB and therefore inhibits inflammatory factors [63]. The short-chain fatty acids produced by intestinal microorganisms act synergistically with IL-22 to enhance the intestinal epithelial barrier's function; *Bifidobacteria* and *Clostridia* stimulate antigen-presenting cells to promote anti-inflammatory IL-10 Treg responses [64]. In the present work, we investigated the differences in the gut microbiota of mice among the control group, DSS group, and DSS with diosmetin group. The alpha diversity index dilution curve of each sample tends to be flat, which indicates that the sequencing result is credible. Alpha diversity index indicated that the microbial diversity in the DSS group remarkably decreased compared with the control group, and the diversity increased and the community composition changed after diosmetin treatment. At the phylum level, the DSS group had an increased ratio of Firmicutes to Bacteroidetes because of the decreased relative abundance of Bacteroidetes and the increased relative abundance of Firmicutes compared with those in the control group. Similar phenomena were found in other studies [13, 65]. However, the DSS with diosmetin group had an increased relative abundance of Bacteroidetes and a decreased abundance of Firmicutes compared with the DSS group.

LEfSe analysis at the OTU level exhibited different dominant bacteria in different groups. *Eggerthella lenta* is a typical bacterium in inflammation [66]. This bacterium was repressed in the DSS with diosmetin group. *Pelomonas* (25%) and *Flavobacterium* (13%) dominate the bacterial composition of patients with high Crohn's DAI, whereas *Bacteroidetes* has a relatively low abundance (4%). In the present study, diosmetin treatment decreased the abundance of *Flavobacterium* and remarkably increased the abundance of Odoribacteraceae*, Prevotella*, Rikenellaceae*, Ruminococcus, Coprococcus, Roseburia, Oscillospira, Anaeroplasma*, *and* Synergistales compared with the DSS group. These bacteria may become potential biomarkers of colitis in the future. These data demonstrated that diosmetin can modulate the community of gut microbiota, especially certain specific microbiomes. These specific bacteria can be beneficial for the treatment of colitis.

CircRNA has emerged as a regulator of many biological processes through the regulation of the circRNA–miRNA–mRNA network [67]. Circ-Sirt1 (hsa_circ_0093887), a member of Sirt1 circRNAs, directly binds to miR-132/212 and interferes with Sirt1 mRNA [25]. Sirt1 plays an important role in anti-inflammation, oxidative stress, and the regulation of gut microbiota. The acetylation of Sirt1 and NF-κB inhibits NF-κB transcription, regulates the key transcription factor of oxidative stress (Nrf2), and therefore affects the redox state of cells. Sirt1 prevents intestinal inflammation by regulating intestinal flora. Sirt1 acts as a transportation hub to monitor the NF-κB and Nrf2 pathways and the intestinal microbiota to maintain intestinal epithelial homeostasis. In this study, the level of circ-Sirt1 was increased by diosmetin in vitro and in vivo, accompanied by the upregulated expression of Sirt1. Subsequently, the acetylation of NF-κB was inhibited, and the Nrf2 pathway was activated. Thus, diosmetin can reverse the effects of si-circSirt1 and si-Sirt1. However, the mechanism of circ-Sirt1 in colitis still needs to be further demonstrated. Our research provides potential research directions for drug development.

In summary, our study demonstrated that diosmetin exerts therapeutic effects in DSS-induced colitis through several pathways, including the reduction of the expression levels of IL-6, IL-1β, IFN-γ, and COX2 and oxidative stress; the increased expression of tight junction proteins (claudin-1, occludin, and ZO-1); and the modulation of gut microbiota. These pathways are partially mediated by diosmetin through the circ-Sirt1/Sirt1 axis. The regulation of gut microbiota composition by diosmetin through Sirt1 still needs further study. Diosmetin can be potentially used to treat colitis or become a lead compound for further optimization.

ACKNOWLEDGEMENTS

This work was financially supported by National Natural Science Foundation of China [Grant 82070060 and 82072660] and the Foundation of Tianjin Pharmaceutical Group Co., Ltd [Grant 735-F1025301].

AUTHOR CONTRIBUTIONS

HLL, YYW, XHL, HGZ, and CY designed the experiments and wrote the manuscript. HLL, YYW, HR, JHL, and SSZ performed the animal and cell experiments. HLL, YYW, and XHL performed the quantitative real-time PCR and Western blotting assays. ZWL and SBS performed the immunofluorescence experiments. RTZ and BWM performed the histopathological section.

ADDITIONAL INFORMATION

Supplementary information The online version contains supplementary material available at https://doi.org/10.1038/s41401-021-00726-0.

Competing interests: The authors declare no competing interests.

REFERENCES

1. da Silva BC, Lyra AC, Rocha R, Santana GO. Epidemiology, demographic characteristics and prognostic predictors of ulcerative colitis. World J Gastroenterol. 2014;20:9458–67.
2. Ungaro R, Mehandru S, Allen PB, Peyrin-Biroulet L, Colombel JF. Ulcerative colitis. Lancet. 2017;389:1756–70.
3. Ordás I, Eckmann L, Talamini M, Baumgart DC, Sandborn WJ. Ulcerative colitis. Lancet. 2012;380:1606–19.
4. Patel H, Barr A, Jeejeebhoy KN. Renal effects of long-term treatment with 5-aminosalicylic acid. Can J Gastroenterol. 2009;23:170–6.
5. Zoubek ME, Pinazo-Bandera J, Ortega-Alonso A, Hernández N, Crespo J, Contreras F, et al. Liver injury after methylprednisolone pulses: a disputable cause of hepatotoxicity. A case series and literature review. United European. Gastroenterol J. 2019;7:825–37.
6. Xu P, Becker H, Elizalde M, Masclee A, Jonkers D. Intestinal organoid culture model is a valuable system to study epithelial barrier function in IBD. Gut. 2018;67:1905–6.
7. Antoni L, Nuding S, Wehkamp J, Stange EF. Intestinal barrier in inflammatory bowel disease. World J Gastroenterol. 2014;20:1165–79.

8. Jäger S, Stange EF, Wehkamp J. Inflammatory bowel disease: an impaired barrier disease. Langenbecks Arch Surg. 2013;398:1–12.
9. Choi W, Yeruva S, Turner JR. Contributions of intestinal epithelial barriers to health and disease. Exp Cell Res. 2017;358:71–77.
10. France MM, Turner JR. The mucosal barrier at a glance. J Cell Sci. 2017;130:307–14.
11. Bourgonje AR, Feelisch M, Faber KN, Pasch A, Dijkstra G, van Goor H. Oxidative stress and redox-modulating therapeutics in inflammatory bowel disease. Trends Mol Med. 2020;26:1034–46.
12. Vaccaro A, Kaplan Dor Y, Nambara K, Pollina EA, Lin C, Greenberg ME, et al. Sleep loss can cause death through accumulation of reactive oxygen species in the gut. Cell. 2020;181:1307–28. e1315
13. Peng Y, Yan Y, Wan P, Chen D, Ding Y, Ran L, et al. Gut microbiota modulation and anti-inflammatory properties of anthocyanins from the fruits of lycium ruthenicum murray in dextran sodium sulfate-induced colitis in mice. Free Radic Biol Med. 2019;136:96–108.
14. Marchesi JR, Adams DH, Fava F, Hermes GD, Hirschfield GM, Hold G, et al. The gut microbiota and host health: a new clinical frontier. Gut. 2016;65:330–9.
15. Hagymási K, Bacsárdi A, Egresi A, Berta E, Tulassay Z, Lengyel G. The role of gut microbiota in chronic liver diseases, and treatment possibilities. Orv Hetil. 2018;159:1465–74.
16. Albillos A, de Gottardi A, Rescigno M. The gut-liver axis in liver disease: pathophysiological basis for therapy. J Hepatol. 2020;72:558–77.
17. McNamara BP, Koutsouris A, O'Connell CB, Nougayréde JP, Donnenberg MS, Hecht G. Translocated espf protein from enteropathogenic escherichia coli disrupts host intestinal barrier function. J Clin Invest. 2001;107:621–9.
18. Li XV, Leonardi I, Iliev ID. Gut mycobiota in immunity and inflammatory disease. Immunity. 2019;50:1365–79.
19. Yeung F, Hoberg JE, Ramsey CS, Keller MD, Jones DR, Frye RA, et al. Modulation of nf-kappab-dependent transcription and cell survival by the sirt1 deacetylase. EMBO J. 2004;23:2369–80.
20. Do MT, Kim HG, Choi JH, Jeong HG. Metformin induces microrna-34a to down-regulate the sirt1/pgc-1α/nrf2 pathway, leading to increased susceptibility of wild-type p53 cancer cells to oxidative stress and therapeutic agents. Free Radic Biol Med. 2014;74:21–34.
21. Wellman AS, Metukuri MR, Kazgan N, Xu X, Xu Q, Ren NSX, et al. Intestinal epithelial sirtuin 1 regulates intestinal inflammation during aging in mice by altering the intestinal microbiota. Gastroenterology. 2017;153:772–86.
22. Ye YL, Yin J, Hu T, Zhang LP, Wu LY, Pang Z. Increased circulating circular rna_103516 is a novel biomarker for inflammatory bowel disease in adult patients. World J Gastroenterol. 2019;25:6273–88.
23. Liu B, Ye B, Zhu X, Yang L, Li H, Liu N, et al. An inducible circular RNA circKcnt2 inhibits ILC3 activation to facilitate colitis resolution. Nat Commun. 2020;11:4076–90.
24. Zhu P, Zhu X, Wu J, He L, Lu T, Wang Y, et al. IL-13 secreted by ILC2s promotes the self-renewal of intestinal stem cells through circular RNA circPan3. Nat Immunol. 2019;20:183–94.
25. Kong P, Yu Y, Wang L, Dou YQ, Zhang XH, Cui Y, et al. circ-Sirt1 controls NF-κB activation via sequence-specific interaction and enhancement of SIRT1 expression by binding to miR-132/212 in vascular smooth muscle cells. Nucleic Acids Res. 2019;47:3580–93.
26. Roowi S, Crozier A. Flavonoids in tropical citrus species. J Agric Food Chem. 2011;59:12217–25.
27. Chen X, Wu Q, Chen Y, Zhang J, Li H, Yang Z, et al. Diosmetin induces apoptosis and enhances the chemotherapeutic efficacy of paclitaxel in non-small cell lung cancer cells via Nrf2 inhibition. Br J Pharmacol. 2019;176:2079–94.
28. Liu Q, Ci X, Wen Z, Peng L. Diosmetin alleviates lipopolysaccharide-induced acute lung injury through activating the Nrf2 pathway and inhibiting the NLRP3 inflammasome. Biomol Ther. 2018;26:157–66.
29. Yang K, Li WF, Yu JF, Yi C, Huang WF. Diosmetin protects against ischemia/reperfusion-induced acute kidney injury in mice. J Surg Res. 2017;214:69–78.
30. Mo GL, He Y, Zhang XQ, Lei X, Luo Q. Diosmetin exerts cardioprotective effect on myocardial ischemia injury in neonatal rats by decreasing oxidative stress and myocardial apoptosis. Clin Exp Pharmacol Physiol. 2020;47:1713–22.
31. Zaragozá C, Villaescusa L, Monserrat J, Zaragozá F, Álvarez-Mon M. Potential therapeutic anti-inflammatory and immunomodulatory effects of dihydroflavones, flavones, and flavonols. Molecules. 2020;25:1017–30.
32. Suzuki K, Sun X, Nagata M, Kawase T, Yamaguchi H, Sukumaran V, et al. Analysis of intestinal fibrosis in chronic colitis in mice induced by dextran sulfate sodium. Pathol Int. 2011;61:228–38.
33. Liu Y, Zhao J, Zhao Y, Zong S, Tian Y, Chen S, et al. Therapeutic effects of lentinan on inflammatory bowel disease and colitis-associated cancer. J Cell Mol Med. 2019;23:750–60.
34. Yang M, Lin HB, Gong S, Chen PY, Geng LL, Zeng YM, et al. Effect of Astragalus polysaccharides on expression of TNF-α, IL-1β and NFATc4 in a rat model of experimental colitis. Cytokine. 2014;70:81–86.
35. Thanou MM, Kotzé AF, Scharringhausen T, Luessen HL, de Boer AG, Verhoef JC, et al. Effect of degree of quaternization of n-trimethyl chitosan chloride for enhanced transport of hydrophilic compounds across intestinal caco-2 cell monolayers. J Control Release. 2000;64:15–25.
36. Sun X, Yang Q, Rogers CJ, Du M, Zhu MJ. AMPK improves gut epithelial differentiation and barrier function via regulating Cdx2 expression. Cell Death Differ. 2017;24:819–31.
37. Wu H, Chen QY, Wang WZ, Chu S, Liu XX, Liu YJ, et al. Compound sophorae decoction enhances intestinal barrier function of dextran sodium sulfate induced colitis via regulating notch signaling pathway in mice. Biomed Pharmacother. 2021;133:110937–51.
38. Puri P, Liangpunsakul S, Christensen JE, Shah VH, Kamath PS, Gores GJ, et al. The circulating microbiome signature and inferred functional metagenomics in alcoholic hepatitis. Hepatology. 2018;67:1284–302.
39. Dai X, Chen X, Chen Q, Shi L, Liang H, Zhou Z, et al. MicroRNA-193a-3p reduces intestinal inflammation in response to microbiota via down-regulation of colonic PepT1. J Biol Chem. 2015;290:16099–115.
40. Wirtz S, Popp V, Kindermann M, Gerlach K, Weigmann B, Fichtner-Feigl S, et al. Chemically induced mouse models of acute and chronic intestinal inflammation. Nat Protoc. 2017;12:1295–309.
41. Rohwer N, Jumpertz S, Erdem M, Egners A, Warzecha KT, Fragoulis A, et al. Non-canonical hif-1 stabilization contributes to intestinal tumorigenesis. Oncogene. 2019;38:5670–85.
42. Li T, Chen RR, Gong HP, Wang BF, Wu XX, Chen YQ, et al. FGL2 regulates IKK/NF-κB signaling in intestinal epithelial cells and lamina propria dendritic cells to attenuate dextran sulfate sodium-induced colitis. Mol Immunol. 2020;117:84–93.
43. Koosha S, Mohamed Z, Sinniah A, Alshawsh MA. Evaluation of anti-tumorigenic effects of diosmetin against human colon cancer xenografts in athymic nude mice. Molecules. 2019;24:2522–33.
44. Su L, Shen L, Clayburgh DR, Nalle SC, Sullivan EA, Meddings JB, et al. Targeted epithelial tight junction dysfunction causes immune activation and contributes to development of experimental colitis. Gastroenterology. 2009;136:551–63.
45. Furuse M, Itoh M, Hirase T, Nagafuchi A, Yonemura S, Tsukita S, et al. Direct association of occludin with ZO-1 and its possible involvement in the localization of occludin at tight junctions. J Cell Biol. 1994;127:1617–26.
46. Saitou M, Furuse M, Sasaki H, Schulzke JD, Fromm M, Takano H, et al. Complex phenotype of mice lacking occludin, a component of tight junction strands. Mol Biol Cell. 2000;11:4131–42.
47. Furuse M, Fujita K, Hiiragi T, Fujimoto K, Tsukita S. Claudin-1 and -2: Novel integral membrane proteins localizing at tight junctions with no sequence similarity to occludin. J Cell Biol. 1998;141:1539–50.
48. Morini J, Babini G, Barbieri S, Baiocco G, Ottolenghi A. The interplay between radioresistant Caco-2 cells and the immune system increases epithelial layer permeability and alters signaling protein spectrum. Front Immunol. 2017;8:223–35.
49. Zhao Y, Guo Q, Zhu Q, Tan R, Bai D, Bu X, et al. Flavonoid VI-16 protects against dss-induced colitis by inhibiting TXNIP-dependent NLRP3 inflammasome activation in macrophages via reducing oxidative stress. Mucosal Immunol. 2019;12:1150–63.
50. Macias-Ceja DC, Cosín-Roger J, Ortiz-Masiá D, Salvador P, Hernández C, Esplugues JV, et al. Stimulation of autophagy prevents intestinal mucosal inflammation and ameliorates murine colitis. Br J Pharmacol. 2017;174:2501–11.
51. Qian J, Jiang F, Wang B, Yu Y, Zhang X, Yin Z, et al. Ophiopogonin d prevents h2o2-induced injury in primary human umbilical vein endothelial cells. J Ethnopharmacol. 2010;128:438–45.
52. Cao YW, Jiang Y, Zhang DY, Wang M, Chen WS, Su H, et al. Protective effects of penthorum chinense pursh against chronic ethanol-induced liver injury in mice. J Ethnopharmacol. 2015;161:92–8.
53. Maejima Y, Kuroda J, Matsushima S, Ago T, Sadoshima J. Regulation of myocardial growth and death by nadph oxidase. J Mol Cell Cardiol. 2011;50:408–16.
54. Biasi F, Astegiano M, Maina M, Leonarduzzi G, Poli G. Polyphenol supplementation as a complementary medicinal approach to treating inflammatory bowel disease. Curr Med Chem. 2011;18:4851–65.
55. Kim TW, Shin JS, Chung KS, Lee YG, Baek NI, Lee KT. Anti-inflammatory mechanisms of koreanaside a, a lignan isolated from the flower of forsythia koreana, against LPS-induced macrophage activation and DSS-induced colitis mice: The crucial role of AP-1, NF-κB, and JAK/STAT signaling. Cells. 2019;8:1163–81. 8
56. Zhang F, Yao S, Yuan J, Zhang M, He Q, Yang G, et al. Elevated IL-6 receptor expression on $CD4^+$ T cells contributes to the increased Th17 responses in patients with chronic hepatitis B. Virol J. 2011;8:270–80.
57. Yamamoto-Furusho JK, Santiago-Hernández JJ, Pérez-Hernández N, Ramírez-Fuentes S, Fragoso JM, Vargas-Alarcón G. Interleukin 1 β (IL-1β) and il-1 antagonist receptor (IL-1rn) gene polymorphisms are associated with the genetic susceptibility and steroid dependence in patients with ulcerative colitis. J Clin Gastroenterol. 2011;45:531–5.

58. Cianciulli A, Calvello R, Cavallo P, Dragone T, Carofiglio V, Panaro MA. Modulation of NF-κB activation by resveratrol in LPS treated human intestinal cells results in downregulation of PGE_2 production and Cox-2 expression. Toxicol Vitr. 2012;26:1122–8.
59. An JH, Li Q, Bhang DH, Song WJ, Youn HY. Tnf-α and inf-γ primed canine stem cell-derived extracellular vesicles alleviate experimental murine colitis. Sci Rep. 2020;10:2115–29.
60. Ni J, Wu GD, Albenberg L, Tomov VT. Gut microbiota and IBD: causation or correlation? Nat Rev Gastroenterol Hepatol. 2017;14:573–84.
61. Zuo T, Kamm MA, Colombel JF, Ng SC. Urbanization and the gut microbiota in health and inflammatory bowel disease. Nat Rev Gastroenterol Hepatol. 2018;15:440–52.
62. Liu F, Smith AD, Solano-Aguilar G, Wang TTY, Pham Q, Beshah E, et al. Mechanistic insights into the attenuation of intestinal inflammation and modulation of the gut microbiome by krill oil using in vitro and in vivo models. Microbiome. 2020;8:83–103.
63. Fang Y, Chen HQ, Zhang X, Zhang H, Xia J, Ding K, et al. Probiotic administration of lactobacillus rhamnosus GR-1 attenuates atherosclerotic plaque formation in $ApoE^{-/-}$ mice fed with a high-fat diet. Eur Rev Med Pharmacol Sci. 2019;23:3533–41.
64. Yang W, Yu T, Huang X, Bilotta AJ, Xu L, Lu Y, et al. Intestinal microbiota-derived short-chain fatty acids regulation of immune cell IL-22 production and gut immunity. Nat Commun. 2020;11:4457–75.
65. Jeffery IB, O'Toole PW, Öhman L, Claesson MJ, Deane J, Quigley EM, et al. An irritable bowel syndrome subtype defined by species-specific alterations in faecal microbiota. Gut. 2012;61:997–1006.
66. Soltys K, Stuchlikova M, Hlavaty T, Gaalova B, Budis J, Gazdarica J, et al. Seasonal changes of circulating 25-hydroxyvitamin d correlate with the lower gut microbiome composition in inflammatory bowel disease patients. Sci Rep. 2020;10:6024–39.
67. Chen LL, Yang L. Regulation of circrna biogenesis. RNA Biol. 2015;12:381–8.